

See discussions, stats, and author profiles for this publication at: <http://www.researchgate.net/publication/281283959>

Quantification of the soil organic carbon balance in the Tai-Lake paddy soils of China

ARTICLE *in* SOIL AND TILLAGE RESEARCH · AUGUST 2015

Impact Factor: 2.58 · DOI: 10.1016/j.still.2015.08.003

8 AUTHORS, INCLUDING:



Qianlai Zhuang

Purdue University

130 PUBLICATIONS 1,100 CITATIONS

SEE PROFILE



Dongsheng Yu

Chinese Academy of Sciences

80 PUBLICATIONS 959 CITATIONS

SEE PROFILE



Xuezheng Shi

Chinese Academy of Sciences

65 PUBLICATIONS 707 CITATIONS

SEE PROFILE

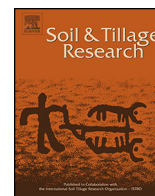


Yaling Liu

Pacific Northwest National Laboratory

17 PUBLICATIONS 14 CITATIONS

SEE PROFILE



Quantification of the soil organic carbon balance in the Tai-Lake paddy soils of China



Guangxiang Wang^a, Liming Zhang^{a,b,c,*}, Qianlai Zhuang^b, Dongsheng Yu^c,
Xuezheng Shi^c, Shihe Xing^a, Dezhong Xiong^a, Yaling Liu^b

^a College of Resource and Environment, Fujian Agriculture and Forestry University, Fuzhou 350002, PR China

^b Department of Earth, Atmospheric, and Planetary Sciences, Purdue University, West Lafayette, IN 47907, USA

^c State Key Laboratory of Soil and Sustainable Agriculture, Institute of Soil Science, Chinese Academy of Sciences, Nanjing 210008, PR China

ARTICLE INFO

Article history:

Received 27 March 2015

Received in revised form 3 August 2015

Accepted 5 August 2015

Keywords:

Soil organic carbon

Paddy soil

DeNitrification–DeComposition (DNDC)

ABSTRACT

Rising temperatures and elevated atmospheric CO₂ are two factors that simultaneously affect the dynamics of soil organic carbon (SOC). This study separately examines the effects arise from these two factors in Tai-Lake Paddy soils using DeNitrification–DeComposition (DNDC) model, with the currently most detailed soil database for the paddy region of China. The soil database is at a scale of 1:50,000, containing 52,034 paddy soil polygons derived from 1107 unique paddy soil profiles. Our simulations indicate that, the SOC in the top soils (0–30 cm) increases 0.83, 1.09, 1.32, and 1.51 Tg C under conventional management (3.44 Tg C) in the 2.32 Mha paddy soils of the Tai-Lake region from 2001 to 2019, respectively, with the atmospheric CO₂ concentration increases at 1.5, 2.0, 2.5, and 3.0 times the normal rate (1.9 ppm year⁻¹). By contrast, with rising air temperature of 0.5, 1.0, 1.5, 2.0, 3.0, and 4 °C, the SOC decreases 0.09, 0.54, 0.69, 1.13, 1.80, and 2.51 Tg C under conventional management, respectively. Thus, the effect of carbon sink induced from CO₂ fertilization at the 2.0 times normal CO₂ concentration increase rate could generally offset the effect of carbon source resulted from a 2.0 °C air temperature increase. In addition, the paddy soils in this region tend to persistently be a sink of atmospheric CO₂ under warming and elevated CO₂ scenarios, even if when the air temperature has increased by 4 °C. These results suggest that SOC storage in paddy soils of this region is prone to benefit from future global climate change and this carbon sequestration potential in the agro-ecosystems is likely to contribute to climate mitigation under current agricultural practices, despite any negative effects derived from warming. As a representative of paddy soils in eastern China, the insights gained from the Tai-Lake region may be potentially transferable to other paddy soils in eastern China where 95% of the total of China is located.

© 2015 Elsevier B.V. All rights reserved.

1. Introduction

Over the past decades, climate change has gained extensive international attention due to the impacts on regional political stability, agriculture, and water supply (Chavas et al., 2009). As for future climate, atmospheric CO₂ concentration and global mean temperature are projected to be increasing. According to IPCC (2013), the global mean temperatures will increase by 0.3 to 4.8 °C by the end of the 21st century. In addition, the increase rate of atmospheric CO₂ concentration has reached 1.9 ppm year⁻¹ for the past decade (IPCC, 2007). While rising temperature causes disappearance of terrestrial carbon sink (Houghton et al., 1998), elevated atmospheric CO₂ can increase SOC content due to

increased plant net primary production (NPP) (Jastrow et al., 2005). Some studies showed that the effect of elevated atmospheric CO₂ on SOC is offset by the effect of climate warming (Lin and Zhang, 2012). However, the counterbalanced magnitudes are still unclear in different terrestrial ecosystems. Understanding the SOC balance between effects induced from rising temperatures and elevated atmospheric CO₂ is therefore crucial for accurate quantification of global carbon budget.

Agro-ecosystem is a highly sensitive part of the global carbon cycle, providing a large potential for carbon sequestration and presenting an immediate viable option for mitigating atmospheric CO₂ (Sun et al., 2010). Previous studies showed that two thirds of the estimated 55 Pg C lost to the atmosphere may be recovered through cultivation of agricultural soils in the next 50–100 years (IPCC 1995; Cole et al., 1996). Rice is the most important agricultural food for more than 50% of the world's population, and it is grown on ~155 Mha of the world's land (Kögel-Knabner

* Corresponding author. Fax: +86 591 83776849.

E-mail address: lmzhang_1979@163.com (L. Zhang).

et al., 2010). China has approximately 38% of the world's rice production and 22% of the world's rice paddies (Wang et al., 1993; Liu et al., 2006). Cultivated for over 7000 years, paddy soils represent a unique type of anthropogenic soil recognized by Chinese soil taxonomy (Li, 1992). Usually, paddy soils may be more promising than upland soil in sequestering C due to the unique water management requirements (Xu et al., 2011). Therefore, the SOC dynamics in paddy soils of China under rising temperatures and elevated atmospheric CO₂ can play a critical role in global greenhouse effect.

Recent years have seen progress in modeling historic patterns and future trends of SOC in agricultural system using process-based models (Álvarez-Fuentes and Paustian, 2011; Gottschalk et al., 2012; Yu et al., 2014). The DeNitrification–DeComposition (DNDC) model simulates the biogeochemical C and N cycle of agricultural soils based on human activity data, land use, soil parameters, daily temperatures, and precipitation (Li et al., 1992a, b). The DNDC has been extensively used to understand the complex interactions among soil management, crop, and climate through integration of the primary SOC turnover mechanisms (Goglio et al., 2014). It has also been used to upscale estimates of SOC changes from sites to regional scales. So far, most of these applications with DNDC were conducted with county- or town-databases that contained relatively coarse soil data with a resolution about 0.5° × 0.5° (Li, 2000; Pathak et al., 2005; Tang et al., 2006; Zhang et al., 2011; Gao et al., 2014). As a result, those simulations using areal average of soil properties ignored the impacts of soil heterogeneity. Additionally, previous studies indicated that the effect of soil properties (e.g. texture, SOC content, bulk density, and pH) on simulating SOC changes at regional scale is a major source of uncertainty for use of DNDC model (Pathak et al., 2005). Recently, a new soil map with improved spatial resolution (1:50,000 scale) became available in the rice-dominated Tai-Lake region of China (Zhang et al., 2012), which allows a refined model estimates by updating soil input parameters.

Given that there are less studies on evaluating the effects of soil heterogeneity and combined effects of rising temperature and CO₂ fertilization on SOC on the soil carbon balance, this study represents a significant step forward to improve the understanding of these effects by linking the currently most detailed 1:50,000 soil database to the DNDC model. The specific objective of this study is to shed light on the SOC balance considering effects of rising temperatures and CO₂ fertilization in the Tai-Lake region, for a better understanding of SOC changes in the context of climate change.

2. Materials and methods

2.1. Study area

The Tai-Lake region (118°50′–121°54′E, 29°56′–32°16′N) is located in the middle and lower reaches of the Yangtze River paddy soil region of China, including part of Jiangsu and Zhejiang provinces and the entire Shanghai City administrative area, with a total area of 36,500 km² (Fig. 1) (Li, 1992). The climate is warm and moist, with annual rainfall of 1100–1400 mm, mean temperature of 16 °C, and average annual sunshine of 1870–2225 h. The frost-free period is over 230 days. The study area, with a long history of rice cultivation spanning several centuries, is one of the oldest agricultural regions in China. Most cropland in the region is managed as a summer rice and winter wheat rotation (Xu et al., 1980).

The paddy soil covers approximately 66% of the total land of this region (Zhang et al., 2012). Paddy soils in the Tai-Lake area are derived mostly from alluvium, loess, and lacustrine deposits.

2.2. Description of the DNDC model

The DNDC model (Version 9.1) was developed in 1992 and has been evolved since then (Li et al., 1992a,b; Li, 2000, 2007a), and it is a process-orientated simulation tool for soil carbon (C) and nitrogen (N) biogeochemistry cycles. It is one of the commonly accepted biogeochemical models in the world, and has been widely used to simulate soil organic carbon (SOC) dynamics and greenhouse gases fluxes (Tang et al., 2006; Tonitto et al., 2007; Abdalla et al., 2011; Xu et al., 2012).

The model consists of six interacting sub-models that describe the generation, decomposition and transformation of organic matter. The sub-models include: (1) soil climate sub-model simulating soil temperature, moisture and redox potential (Eh) profiles and soil water fluxes through time based on soil physical properties, weather, and plant water use; (2) nitrification sub-model tracking growth of nitrifiers and turnover of NH₄⁺; (3) denitrification sub-model calculating hourly denitrification rates and N₂, NO and N₂O production during periods when the soil Eh decreases due to the rainfall, irrigation, soil flooding or freezing; (4) decomposition sub-model simulating decomposition of the SOC pools and CO₂ production by soil microbes and NH₃ volatilization; (5) plant growth sub-model driven by the air temperature and soil water and N availability at daily time steps by tracking photosynthesis, respiration, water and N demand, C allocation, crop yield, and litter production; and (6) fermentation sub-model quantifies daily methane (CH₄) production, oxidation, and transport.



Fig. 1. Geographical location of the study area in China.

Because existing input data (e.g., management practice data and meteorological data) were often limited to county level, county was used as the basic simulation unit by default in regional simulations in the DNDC model (Li et al., 2004), despite of any heterogeneity in land surface characteristics and soil properties within one specific county. As a result, the model estimates are highly uncertain due to missing information of soil heterogeneity within counties (Zhang et al., 2014). In this study, however, soil-type-specific polygon was used as the basic simulation unit of the DNDC model to take advantage of the spatially explicit soil information. The SOC estimates are for the top 0–30 cm soils (Tang et al., 2006). More complete discussion of DNDC model validation for this region can be found in Zhang et al. (2012).

2.3. Data

We collected soil properties, cropping systems, daily weather, and agricultural management practices as input data for DNDC, to simulate SOC changes in the rice paddy area in the Tai-Lake region.

A 1:50,000 polygon-based soil database was developed to drive the DNDC model for regional simulations. The polygonal soil database containing 52,034 paddy soil polygons was derived from 1107 unique paddy soil profiles, which were collected during the second national soil survey of China in the 1980s–1990s. According to the genetic soil classification of China (GSCC) system, paddy soils are classified into 6 soil subgroups, 137 soil families and 622 soil species, which are represented in the 1:50,000 digital soil map (Shi et al., 2006; Zhang et al., 2012). The 6 soil subgroups in GSCC nomenclature based on the US Soil Taxonomy (ST) include: submergenic (typic endoaquepts), hydromorphic (typic epiaquepts), gleyed (typic endoaquepts), bleached (typic epiaquepts), degleyed (typic endoaquepts), and pergenic (typic epiaquepts) (Shi et al., 2006; Soil Survey Staff, 2010). The soil attributes assignment in the soil database was compiled using the pedological knowledge based (PKB) method based on GSCC (Zhao et al., 2006; Yu et al., 2007). This database contains many soil attributes including soil name, horizon thickness, clay content, organic carbon content, bulk density, and pH.

In this study, a dataset of crop types including physiological data for summer rice and winter wheat at the county level was also used. The target domain covered 37 counties in the Tai-Lake region. The crop parameters for rice–wheat rotation system were obtained from a thorough sample testing. A complete description of information can be found in Gou et al. (1999) and Li (2007a,b).

Daily precipitation, maximum and minimum air temperature for 1982–2000 from 13 weather stations in the Tai-Lake region was obtained from the China Meteorological Administration (China Meteorological Administration, 2011). Climate data of the nearest weather station was assigned to each county in model simulations.

Farming management in the study area included (1) fertilizer application: the application rate of livestock and human manure at the county level was obtained from the Resources and Environmental Scientific Data Center, Chinese Academy of Sciences (Xu et al., 2012). 20% of livestock manure and 10% of human manure

was applied twice as base fertilizer for rice and wheat, where the total manure amount is estimated from population (866, 44, 95, and 23 kg C head⁻¹ year⁻¹ for cattle, sheep, swine and human, respectively) (Lu and Shi, 1982., Tang et al., 2006). N synthetic fertilizer was applied three in the basal, tillering and heading stages for rice and three times in the basal, jointing and heading stages for wheat; (2) water management: 5 times of shallow flooding and one time of midseason were applied for summer rice; (3) tillage: till to a depth of 20 cm during planting for rice and no-till for wheat; (4) crop residue management: 15% of non-grain post harvest crop biomass was returned to soil (Gou et al., 1999; Tang et al., 2006; Zhang et al., 2014).

2.4. Scenarios of temperatures and CO₂ concentrations

In the baseline scenario, we assume that the management practices in 2000 have been continuously used until 2019. Alternative scenarios were compiled by changing one of the two climatic factors of air temperatures or atmospheric CO₂ concentrations based on the baseline scenario (Table 1). According to the available meteorological data, the recent 19-year climate data of 1982–2000 was repeatedly used for the period 2001–2019 for all scenarios runs (Xu et al., 2011). The baseline and alternative scenarios use the same soil and crop data.

2.5. Data Analysis

Area of paddy soils (APS, ha), average annual SOC change (AASC, kg C ha⁻¹ year⁻¹) and total SOC change (TSC, Tg C or Gg C) for the Tai-Lake region were calculated using Eqs. (1)–(4), respectively:

$$APS = \sum_{i=1}^n APS_i \quad (1)$$

$$AMSC = \sum_{f=1}^h ASC_f \quad (2)$$

$$TSC = \sum_{i=1}^n (APS_i \times AMSC_i) \quad (3)$$

$$AASC = TSC/APS/19 \quad (4)$$

where APS_i is the area of i -th polygon of paddy soil; ASC_f (kg C ha⁻¹ year⁻¹) is the annual SOC change in a specific polygon, as estimated by the DNDC modeling; $AMSC_i$ (kg C ha⁻¹ year⁻¹) is the accumulated annual SOC change in a specific polygon from 2001 to 2019; n is the polygon number; and h is the order of simulation years from 2001 to 2019 ($h = 1, 2, 3 \dots 19$).

The SOC increase (or decrease) amount (y , kg C ha⁻¹ year⁻¹) of alternative scenarios was calculated with Eq. (5):

$$y = X_s - X_0 \quad (5)$$

Table 1
Baseline and alternative scenarios in the Tai-Lake region.

Scenario	Conditions or variations
Baseline (Conventional management, CT)	Rice–wheat rotation, 15% of above-ground crop residue incorporated in soil after harvest, 20 cm tilling depth for rice of conventional tillage and no-till was applied for wheat, one time of midseason and intermittence irrigation (shallow flooding) were applied at summer rice, manure of 20% of livestock wastes and 10% of human wastes, N concentration in the atmosphere was stabilized at 379 ppm.
CO ₂ concentration	Climatic Factor
Air temperature	Increasing at 1.5, 2.0, 2.5, and 3.0 times the normal increase rate (1.9 ppm year ⁻¹) (1.5CT, 2.0CT, 2.5CT, and 3.0CT, respectively). Increase by 0.5, 1.0, 1.5, 2.0, 3.0, and 4 °C (T0.5, T1, T1.5, T2, T3, and T4, respectively).

where X_0 is the AASC of conventional management under the baseline, and X_s is the AASC of alternative scenarios.

In order to test the most sensitive soil properties factor affecting SOC, the correlation between average annual SOC change and soil properties was determined by step-wise regression analysis via statistical package for social sciences (SPSS) statistical software (Leech et al., 2008).

3. Results and discussion

3.1. Annual variation of SOC changes in the Tai-lake region

3.1.1. Effects of elevated CO_2

The model results indicated that SOC balance was positive under conventional management (CT) and elevated atmospheric CO_2 in the 2.32 Mha paddy soils of the Tai-Lake region from 2001 to 2019 (Fig. 2). When the atmospheric CO_2 concentration increases at 1.5, 2.0, 2.5, and 3.0 times the normal rate (1.9 ppm $year^{-1}$) (1.5CT, 2.0CT, 2.5CT, and 3.0CT, respectively), the total SOC changes in the top soils (0–30 cm) were 4.27, 4.53, 4.76, and 4.95 Tg C, respectively, from 2001–2019 (Table 2). The corresponding average annual SOC changes were 97, 103, 108, and 112 kg C $ha^{-1} year^{-1}$, respectively. These results are consistent with the current management practices in this region. High rate use of fertilizer (335 kg N $ha^{-1} year^{-1}$) and farmyard manure (270 kg C $ha^{-1} year^{-1}$) and return of crop residue to soils in this region is likely to increase SOC. Additionally, no-tillage practice has been extensively implemented in this region when planting wheat (Zhang et al., 2012). This practice limits soil disturbance and hence restrains SOC decomposition (Li et al., 2006). The SOC changes of the 1.5CT, 2.0CT, 2.5CT, and 3.0CT scenarios would be 24.04, 31.70, 38.13, and 43.87% higher, respectively, relative to the baseline scenario (Table 2). Aside from management practices, another reason is induced from increased vegetation production—enrichment of atmospheric CO_2 could increase production of vegetation (Fuhrer, 2003; Booker et al., 2005), consequently, more organic carbon was fed to the soil carbon pools, resulting in SOC increase (Lin and Zhang, 2012).

The inter-annual variations in the modeled annual SOC change are large (Fig. 2). From 2001–2008, the SOC increasing rate slowed down under conventional management and elevated atmospheric CO_2 scenarios. According to agricultural statistical data, the amounts of synthetic fertilizer and farmyard manure use in the region slightly decreased since 1996 (Zhang et al., 2009b). The modeled results are in agreement with many reports that indicated

the annual SOC sequestration rate of Chinese rice paddies was flat or has declined since the mid-1990s (Zhang et al., 2007; Xu et al., 2012). Additionally, climate change could play a role in the long-term SOC change trend as well. The annual precipitation increased from 2001 to 2008 (Fig. 3). Some studies indicated that the precipitation in this region was negatively correlated with the SOC sequestration rate significantly (Bu, 2013). High precipitation can reduce crop yields and biomass production by causing N leaching to deeper soil layers (Peinetti et al., 2008), consequently, less organic matter was fed to the soil carbon pools.

However, the SOC increasing rate increased and reached a stable level for the period of 2009–2019 (Fig. 2). This is because the loss of organic matter during the period of 2001–2008 led to lower SOC equilibriums (Gaston et al., 1993). Subsequently, the SOC content will gradually increased because soils with lower initial SOC displayed greater SOC increase potential due to low decomposition rate (Zhao et al., 2013). Furthermore, the annual rainfall in the Tai-Lake region slightly decreased during the same study period; as opposed to increase of annual mean temperature (Fig. 3). Low mean annual precipitation is linked to high SOC increasing rate (Peinetti et al., 2008). In contrast, rising temperatures could cause decrease of vegetational production, and consequently reduce the SOC due to reduced C input into the soil carbon pools (Gaumont-Guay et al., 2006). The positive effects derived from decreasing precipitation were then offset by the negative effects induced by warming. Consequently, the SOC increasing rates under conventional management and elevated atmospheric CO_2 scenarios reached a stable level during the period of 2013–2019 (Fig. 2).

3.1.2. Effects of increased temperature

SOC decreased with rising temperature and it was sensitive to temperature changes (Fig. 4). With rising air temperature of 0.5, 1.0, 1.5, 2.0, 3.0, and 4 °C (T0.5, T1, T1.5, T2, T3, and T4, respectively), the total SOC changes during 2001–2019 in paddy soil of the Tai-Lake region were 3.35, 2.90, 2.75, 2.31, 1.64, and 0.92 Tg C, respectively. The corresponding average annual SOC changes were 76, 66, 62, 52, 37, and 21 kg C $ha^{-1} year^{-1}$, respectively (Table 3). The SOC changes under T0.5, T1, T1.5, T2, T3, and T4 scenarios would be 2.72, 15.87, 20.17, 32.82, 52.43, and 73.13% lower, respectively, than the baseline scenario. The main reason was that rising temperature accelerates plant growth, shortens grain-fill period (Fuhrer, 2003). In addition, warmer conditions enhance soil N availability through higher rates of mineralization

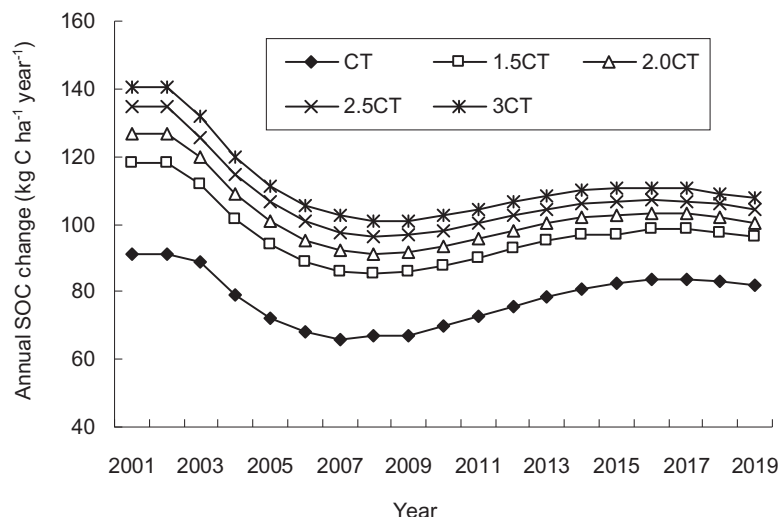


Fig. 2. Annual SOC changes under conventional management and elevated atmospheric CO_2 scenarios from 2001 to 2019 in the Tai-Lake region, China.

Table 2

Average annual SOC change (AASC, $\text{kg C ha}^{-1} \text{ year}^{-1}$) and the total SOC change during 2001–2019 (TSC, Tg C) under different atmospheric CO_2 concentrations scenarios, and at whole Tai-Lake region, soil subgroups, sub-regions and administrative areas spatial levels.

	Areas 10^4 ha	CT		1.5CT		2.0CT		2.5CT		3.0CT	
		AASC	TSC	AASC	TSC	AASC	TSC	AASC	TSC	AASC	TSC
Whole Tai-Lake region											
Tai-Lake region	232.02	78	3.44	97	4.27	103	4.53	108	4.76	112	4.95
Soil subgroups											
Bleached	20.22	203	0.79	219	0.85	223	0.87	227	0.88	231	0.90
Gleyed	10.17	-144	-0.28	-120	-0.23	-112	-0.22	-108	-0.21	-104	-0.20
Percogenic	37.16	209	1.48	229	1.61	235	1.66	240	1.70	245	1.73
Degleyed	40.96	-81	-0.63	-62	-0.49	-56	-0.44	-51	-0.40	-46	-0.36
Submergenic	0.73	253	0.035	269	0.037	275	0.038	280	0.039	284	0.040
Hydromorphic	122.56	88	2.05	107	2.48	113	2.62	118	2.74	122	2.85
Sub-regions											
Rolling hills	39.47	112	0.84	130	0.98	135	1.01	140	1.05	144	1.08
Plains around the lake	59.31	45	0.50	61	0.69	67	0.75	70	0.79	75	0.84
Plains along the river	63.79	195	2.36	217	2.63	224	2.72	231	2.79	236	2.85
Polders	69.46	-20	-0.27	-2	-0.02	4	0.06	9	0.12	13	0.18
Administrative areas											
Jiangsu province	132.63	102	2.56	119	3.01	125	3.15	129	3.26	134	3.37
Zhejiang province	53.84	-0.11	-0.0011	18	0.18	24	0.25	29	0.29	34	0.35
Shanghai City	45.55	101	0.88	124	1.08	131	1.13	138	1.20	143	1.24

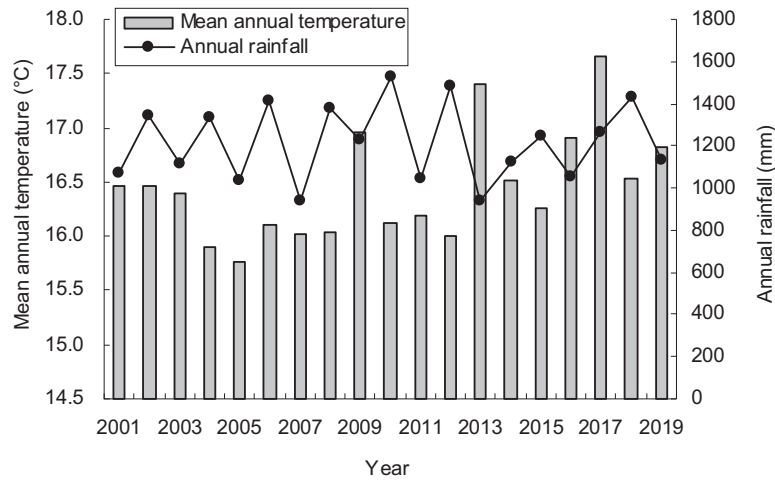
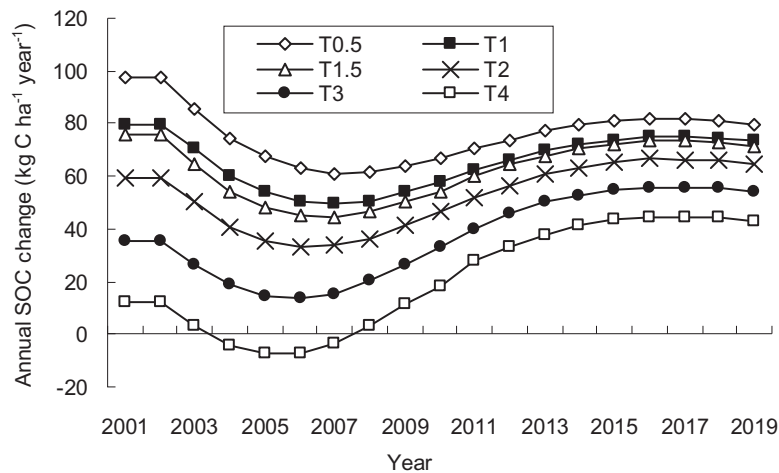
**Fig. 3.** Variations of annual rainfall and annual mean temperature from 2001 to 2019 in the Tai-Lake region, China.**Fig. 4.** Annual SOC changes under different rising temperature scenarios from 2001 to 2019 in the Tai-Lake region, China.

Table 3
Average annual SOC change (AASC, kg C ha⁻¹ year⁻¹) and the total SOC change (TSC, Tg C) during 2001–2019 under different rising temperature scenarios, and at whole Tai-Lake region, soil subgroups, sub-regions and administrative areas spatial levels.

	T0.5		T1		T1.5		T2		T3		T4	
	AASC	TSC	AASC	TSC	AASC	TSC	AASC	TSC	AASC	TSC	AASC	TSC
Whole Tai-Lake region	76	3.35	66	2.90	62	2.75	52	2.31	37	1.64	21	0.92
Tai-Lake region	76	3.35	66	2.90	62	2.75	52	2.31	37	1.64	21	0.92
Soil subgroups												
Bleached	208	0.81	198	0.77	198	0.77	190	0.74	178	0.69	166	0.64
Gleyed	-149	-0.29	-166	-0.32	-172	-0.33	-189	-0.36	-218	-0.42	-235	-0.46
Percogenic	208	1.47	202	1.42	199	1.40	193	1.36	181	1.28	170	1.20
Degleyed	-85	-0.66	-98	-0.77	-103	-0.81	-115	-0.90	-133	-1.03	-149	-1.16
Submergenic	249	0.035	251	0.035	240	0.033	233	0.032	220	0.031	200	0.028
Hydromorphic	85	1.99	75	1.76	72	1.68	62	1.45	47	1.10	29	0.67
Sub-regions												
Low mountain and hilly	108	0.81	102	0.76	96	0.72	88	0.66	72	0.54	55	0.41
Tai-Lake plain	45	0.51	34	0.38	33	0.37	21	0.24	5	0.05	-9	-0.10
Alluvial plain	193	2.34	185	2.24	182	2.21	175	2.12	165	1.99	147	1.79
Polders	-24	-0.31	-37	-0.49	-42	-0.55	-53	-0.71	-72	-0.95	-88	-1.17
Administrative areas												
Jiangsu province	101	2.55	92	2.32	89	2.24	79	1.98	63	1.58	49	1.24
Zhejiang province	-6	-0.057	-18	-0.18	-22	-0.23	-34	-0.35	-50	-0.51	-68	-0.69
Shanghai City	99	0.85	88	0.76	85	0.73	78	0.68	66	0.57	44	0.38

(Parton et al., 1995), meanwhile, it also induce higher system N losses if N demand by the plant is not synchronized with N supply (Fuhrer, 2003). These effects reduce production of vegetation, and consequently reduce SOC due to decreased input into the soil carbon pools. In addition, climate warming also elevates soil temperature, and stimulates SOC decomposition (Gaumont-Guay et al., 2006).

As can be seen from the Fig. 4, the modeled annual SOC changes highly varied from year to year under different rising temperature scenarios. A particularly noteworthy problem was that the lowest values of annual SOC change under different rising temperature scenarios were found in 2006, earlier than that in the conventional management and elevated atmospheric CO₂ scenarios (Figs. 2 and 4). It also demonstrates that the type of environmental factor employed (i.e. elevated CO₂ concentration, rising temperature, etc.) can significantly affect the time required to reach a new equilibrium level of organic carbon in soil (Gaston et al., 1993; Xu et al., 2012).

The positive effect of elevated atmospheric CO₂ on SOC might be counter balanced by the negative effect of climate warming (Wang et al., 2007). Our model results indicate that, taking the average annual SOC change (78 kg C ha⁻¹ year⁻¹) of CT scenario as the baseline, the SOC increase amount (25 kg C ha⁻¹ year⁻¹) by rising atmospheric CO₂ concentration to 2.0 times normal increase

rate could almost offset the SOC decrease amount (26 kg C ha⁻¹ year⁻¹) by rising temperature to 2.0 °C (Tables 2 and 3). This is generally consistent with previous studies. For example, Lin and Zhang, (2012) found that the effect of elevated CO₂ on SOC was approximately balanced by that of warming 2 °C at the Nelson Farm of Mississippi, USA. In addition, the paddy soils in this region tend to constantly be a sink of atmospheric CO₂ under warming and elevated CO₂ scenarios, even if the air temperature increased to 4 °C (Figs. 2 and 4). Paddy soils in the Tai-Lake region are recognized as the most typical of their type in China (Xu et al., 1980). Therefore, our research results provide an effective reference for other regions of China (Li, 1992). Further, our findings suggest that SOC storage in paddy soils of China is prone to benefit from future global climate change and this carbon sequestration potential in the agro-ecosystems is likely to contribute to climate mitigation under current agricultural practices, despite the negative effects of warming.

3.2. Comparison of SOC change for different paddy soil subgroups

The effects of rising temperature and CO₂ fertilization on potential soil C sequestration were significantly dependent on paddy soil subgroups (Tables 2 and 3). The subgroup of hydromorphic soil covers about 1.23 Mha and accounts for 53%

Table 4
Individual contributions of major soil properties to the variations of average annual SOC change in Tai-Lake region paddy soils from 2001 to 2019.

Scenario	Number of simulation units	ΔR^{2a}				Adjusted R ²
		Initial SOC (g kg ⁻¹)	Clay (%)	pH	Bulk density (g cm ⁻³)	
CT	52,034	0.730***	0.086***	0.056***	0.004***	0.876***
1.5CT		0.708***	0.089***	0.058***	0.004***	0.859***
2.0CT		0.718***	0.086***	0.056***	0.004***	0.865***
2.5CT		0.691***	0.101***	0.061***	0.005***	0.857***
3.0CT		0.711***	0.087***	0.056***	0.004***	0.859***
T0.5		0.732***	0.084***	0.056***	0.004***	0.876***
T1		0.735***	0.080***	0.057***	0.003***	0.875***
T1.5		0.733***	0.078***	0.058***	0.003***	0.872***
T2		0.735***	0.073***	0.058***	0.004***	0.870***
T3		0.740***	0.067***	0.057***	0.004***	0.868***
T4		0.747***	0.065***	0.053***	0.004***	0.869***

*** significant at 0.001 probability levels, respectively.

^a The change in the R² statistic is produced by adding a soil property into stepwise multiple regressions.

of the total paddy soil area in the Tai-Lake region (Table 2). As Table 4 illustrated, initial SOC content and clay content under rising temperatures and elevated atmospheric CO₂ scenarios were the most sensitive parameters controlling SOC change among all soil factors. Initial SOC content accounted for 69.1–74.7% of the variations in average annual SOC change for paddy soils from 2001 to 2019, and clay content accounted for 6.5–10.1% of the variations. While soils with higher clay content possesses a greater capacity to protect SOC and stabilize soil conditions (Six et al., 2002; McLauchlan, 2006), soil with lower initial SOC displays a higher rate of SOC accumulation due to the low decomposition rate (Zhao et al., 2013). As a result, hydromorphic paddy soils that possess relatively high clay (28%) and low initial SOC (15.4 g kg⁻¹) (Table 5) have large potential for carbon sequestration. The modeled total SOC changes under 1.5CT, 2.0CT, 2.5CT, and 3.0CT scenarios in hydromorphic paddy soils ranged from 2.48–2.85 Tg C from 2001 to 2019, with higher carbon sink potential occurring in higher CO₂ concentration scenarios (Table 2). In contrast, the ability of carbon sequestration in hydromorphic paddy soils obviously decreased when the temperature rises, and total SOC changes ranged from 1.99–0.67 Tg C along with 0.5–4 °C rise in temperature (Table 3).

The percogetic paddy soils, bleached paddy soils, and submergenic paddy soils accounted for 16, 8.8 and 0.32% of the total paddy soil area in the Tai-Lake region, respectively (Table 2). The modeled total SOC changes under 1.5CT, 2.0CT, 2.5CT, and 3.0CT scenarios in the period 2001–2019 ranged from 1.61–1.73 Tg C in percogetic paddy soils, 0.85–0.90 Tg C in bleached paddy soils, and 0.037–0.040 Tg C in submergenic paddy soils (Table 2). The modeled total SOC changes under T0.5, T1, T1.5, T2, T3, and T4 scenarios in the period 2001–2019 ranged from 1.20–1.42 Tg C in percogetic paddy soils, 0.64–0.77 Tg C in bleached paddy soils, and 0.028–0.035 Tg C in submergenic paddy soils. These three paddy soil subgroups present the potential of strong carbon sink under warming and elevated atmospheric CO₂ scenarios, which is mainly due to relatively low initial SOC content, relatively high average chemical fertilizer application rate and clay content (in percogetic paddy soils), and acidic pH value (in bleached paddy soils) (Table 5) (Pacey and DeGier, 1986; Li et al., 2004; Brar et al., 2013).

The gleyed paddy soils and degleyed paddy soils accounted for 4.4 and 18% of the total paddy soil area in the Tai-Lake region, respectively (Table 2). In contrast to other subgroups, the SOC

balance of these two subgroups was negative under rising temperatures and elevated atmospheric CO₂ scenarios. The modeled total SOC changes of 1.5CT, 2.0CT, 2.5CT, and 3.0CT in the period 2001–2019 ranged from –0.20–0.23 Tg C in gleyed paddy soils, and –0.36 Tg C–0.49 Tg C in degleyed paddy soils (Table 2). Likewise, the modeled total SOC changes of T0.5, T1, T1.5, T2, T3, and T4 in the period 2001–2019 ranged from –0.29–0.46 Tg C in gleyed paddy soils, and –0.66–1.16 Tg C in degleyed paddy soil (Table 3). The main reason was that these two paddy soil subgroups possessed relatively high initial SOC contents and mean annual temperatures (Table 5). Moreover, the pH value of gleyed paddy soils was closer to neutral (Table 5). High mean annual temperature and neutral pH value are often linked to accelerated soil decomposition and high CO₂ emissions (Pacey and DeGier, 1986; Gaumont-Guay et al., 2006).

Overall, the SOC changes under rising temperatures and elevated atmospheric CO₂ scenarios vary substantially from subgroup to subgroup, due to prominent heterogeneity in soil properties across different soil subgroups. Especially, small variations in the initial SOC content would cause large changes in CO₂ emission. This emphasizes the importance of detailed and finer scale soil database (e.g., 1:50,000) in estimating the SOC balance between rising temperatures and elevated atmospheric CO₂ in the future. In addition, our results also suggest the necessity of tailoring management practices for different soil subgroups to increase the potential of carbon sink or restrain the potential of carbon source in the context of future global climate change. For example, although the management measure of continuous flooding was applied to the gleyed soils (Zhang et al., 2009a), the SOC balance was still negative under rising temperatures and elevated atmospheric CO₂ scenarios. Effective on-farm management measures (e.g., no-tillage, synchronization of nutrition and water needs, and straw and manure application) should be introduced to enhance soil carbon storage and march toward warming mitigation (Xu et al., 2011).

3.3. Comparison of SOC change between different paddy soil sub-regions

There are four sub-regions classified by the characteristics of landscape and soils in Tai-lake region: alluvial plain, low mountain and hilly, Tai-Lake plain, and polders (Fig. 5) (Xu et al., 1980).

Table 5

Model input of soil properties, climatic factors and fertilizer amount at whole Tai-Lake region, soil subgroups, sub-regions and administrative areas spatial levels.

	Soil properties				Climatic factors		Fertilizer amount	
	Initial SOC (g kg ⁻¹)	Clay (%)	pH	Bulk density (g cm ⁻³)	Annual mean rainfall (mm)	Mean annual temperature (°C)	Fertilizer (kg N ha ⁻¹ year ⁻¹)	Manure (kg C ha ⁻¹ year ⁻¹)
Whole Tai-Lake region	15.4	26	6.7	1.18	1216	16.4	335	270
Tai-Lake region	15.4	26	6.7	1.18	1216	16.4	335	270
	Soil subgroups							
Bleached	10.4	16	6.1	1.20	1153	16.4	302	188
Gleyed	24.8	35	7.1	1.00	1209	16.6	363	223
Percogetic	11.5	22	6.9	1.22	1147	16.3	369	237
Degleyed	19.3	30	6.5	1.20	1256	16.7	351	308
Submergenic	10.4	15	6.8	1.10	1179	15.2	281	164
Hydromorphic	15.4	28	6.7	1.17	1234	16.4	323	287
	Sub-regions							
Low mountain and hilly	13.4	22	6.0	1.18	1270	15.6	284	186
Tai-Lake plain	15.6	24	6.6	1.19	1154	16.5	296	215
Alluvial plain	13.4	27	7.2	1.19	1213	16.7	395	350
Polders	18.2	30	6.5	1.15	1241	16.7	293	343
	Administrative areas							
Jiangsu province	14.2	25	6.5	1.19	1156	16.5	311	184
Zhejiang province	17.9	29	6.3	1.14	1386	16.1	309	319
Shanghai city	16.1	26	7.4	1.17	1189	16.8	436	464

The value of all factors is weighted average by the area of each polygon.

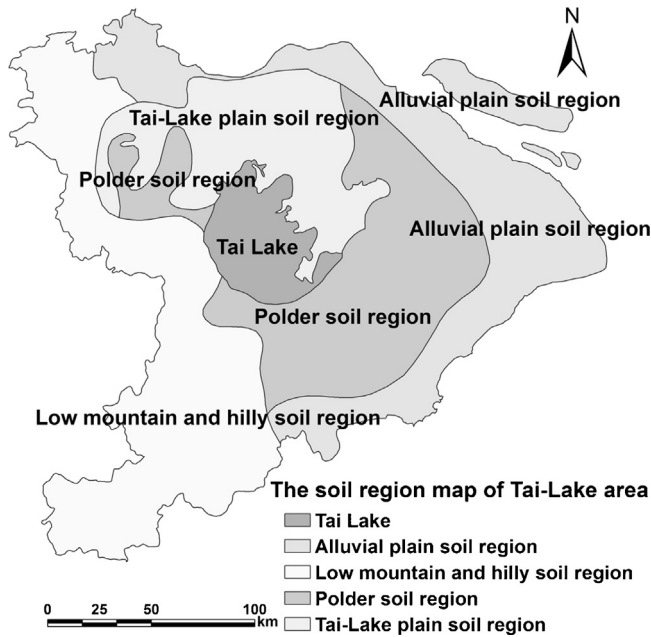


Fig. 5. Paddy soil region map of the Tai-Lake region, China.

The SOC sequestration rate in the Tai-Lake plain sub-region was lower than that of the alluvial plain, and low mountain and hilly sub-regions under rising temperatures and elevated atmospheric CO₂ scenarios (Figs. 6 and 7), due to the higher initial SOC content

and lower clay content (Table 5) (Li et al., 2004). Taking the average annual SOC change of CT scenario as the baseline, the SOC increase by rising atmospheric CO₂ concentration to 2.5 times normal increase rate in the Tai-Lake plain sub-region could almost offset the SOC decrease by rising temperature to 2.0 °C (Tables 2 and 3). The requirement of a 2.5 times normal increase rate in CO₂ concentration in this sub-region, relative to 2.0 times in the entire Tai-Lake region (see Section 3.1), to offset the effects of a 2.0 °C temperature increase suggests that the joint effects of these two factors on SOC balance are highly variable across the Tai-Lake region. Therefore, our results suggest that it is necessary to identify the SOC fate resulted from counteracting effects of rising temperatures and elevated atmospheric CO₂ in other major rice production regions of China, so as to facilitate sound policy making that aims at SOC increase and climate mitigation.

The SOC sequestration rate in the alluvial plain sub-region under rising temperatures and elevated atmospheric CO₂ was the highest among the four sub-regions (Figs. 6 and 7), due to the highest application rates of fertilizer and manure (Table 5). By contrast, the average annual SOC change in the polder sub-region was the lowest under warming and elevated atmospheric CO₂ scenarios (Figs. 6 and 7), due to the highest of initial SOC content and annual average temperature (Table 5) (Gaumont-Guay et al., 2006).

The modeled results at soil sub-region scales indicated that the C sequestration rate under rising temperatures and elevated atmospheric CO₂ scenarios is greatly influenced by the most sensitive soil factors (e.g., clay content and initial SOC) in addition to environmental factors, with greater retention of

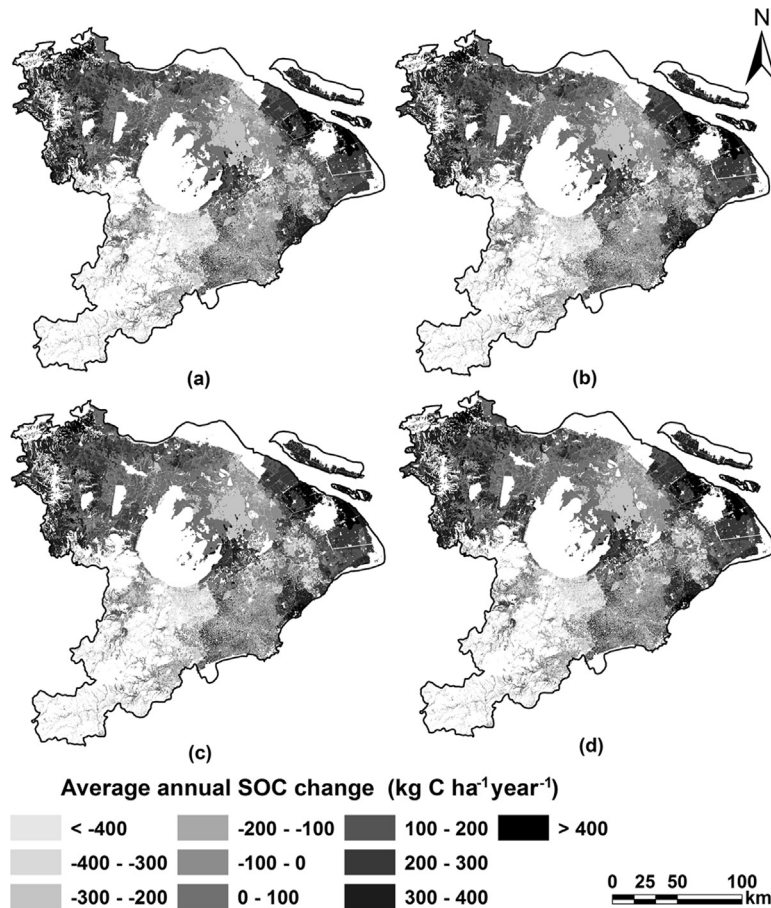


Fig. 6. Spatial distribution of average annual SOC change under different atmospheric CO₂ concentrations scenarios in the Tai-Lake region, China: (a) 1.5CT; (b) 2.0CT; (c) 2.5CT; (d) 3.0CT.

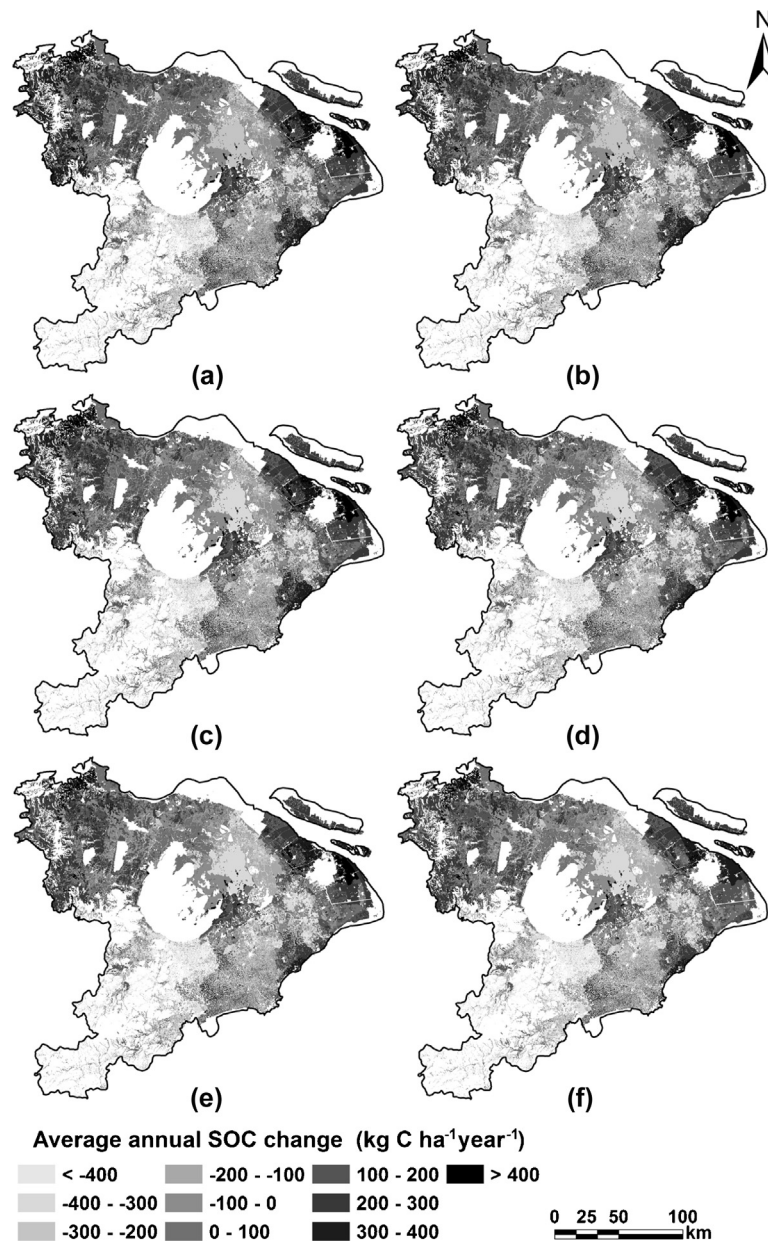


Fig. 7. Spatial distribution of average annual SOC change under different rising temperature scenarios in the Tai-Lake region, China: (a) T0.5; (b) T1; (c) T1.5; (d) T2; (e) T3; (f) T4.

added C in soils having a higher clay content and lower initial SOC value (Tables 2, 3 and 5); this is recognized in models such as RothC (Coleman et al., 1997) and CENTURY (Parton et al., 1993). Therefore, accurate information of these soil factors as model inputs are critical to reducing the uncertainties in model results.

3.4. Comparison of SOC change between different administrative areas

There are 1.33, 0.54 and 0.46 Mha of paddy soils of the Tai-Lake region distributed in Jiangsu, Zhejiang Province and Shanghai City administrative area. The SOC changes vary significantly from area to area under warming and elevated atmospheric CO₂ scenarios (Tables 2 and 3). Either under elevated atmospheric CO₂ concentration or warming scenarios, the average annual SOC changes of Jiangsu Province and Shanghai City was apparently higher than that of Zhejiang Province. This is likely because the initial SOC in Jiangsu Province and Shanghai City were lower, plus

that the fertilizer and manure use rate in Shanghai City were higher (Table 5) (Li et al., 2004; Brar et al., 2013).

By looking at SOC changes at county scale, 24 counties gained SOC and 12 counties lost SOC from 2001 to 2019 in different atmospheric CO₂ concentration scenarios (Table 6). A particularly noteworthy result was that the Linan County of CT and 1.5CT scenario were a weak carbon source in the period of 2001–2019. However, the SOC balance of 2.0CT, 2.5CT, and 3.0CT in Linan County were positive with average annual changes ranging from 2.0 to 21 kg C ha⁻¹year⁻¹ during the same study period. The simulation suggested that the effect of elevated atmospheric CO₂ may cause an ecosystem shift between carbon source and sink (Lin and Zhang, 2012).

The model results at county scale indicated that SOC response tends to be more sensitive to warming than elevated atmospheric CO₂ (Table 7). For example, the high SOC decrease amount of different temperature scenarios occurred in the Jiading (3.0 –148 kg C ha⁻¹year⁻¹), Wu County (5.0 –91 kg C ha⁻¹year⁻¹),

Table 6
Average annual SOC change (AASC, kg C ha⁻¹ year⁻¹) and the total SOC change (TSC, Gg C) under different atmospheric CO₂ concentration scenarios by county level in the Tai-Lake region during the period of 2001–2019, China.

County	Areas 10 ⁴ ha	CT		1.5CT		2.0CT		2.5CT		3.0CT	
		AASC	TSC	AASC	TSC	AASC	TSC	AASC	TSC	AASC	TSC
Wuxian	14.78	-114	-320	-88	-246	-79	-221	-74	-208	-67	-189
Zhangjiagang	2.54	76	37	88	42	91	44	95	46	98	47
Changshu	7.55	-103	-148	-90	-129	-87	-125	-82	-118	-80	-115
Taicnang	6.14	181	211	208	243	216	252	226	263	231	270
Kunshan	7.57	-93	-133	-82	-118	-79	-113	-76	-109	-73	-105
Wujiang	9.79	148	275	171	319	180	335	185	343	190	354
Wuxi	9.77	31	58	43	81	47	87	49	91	52	97
Jiangyin	8.69	101	167	114	189	120	199	124	205	128	212
Wujin	14.85	73	267	104	293	108	306	110	312	114	321
Jintan	7.1	185	250	199	268	203	273	207	279	209	282
Liyang	10.84	201	415	218	449	221	455	226	465	227	469
Yixing	10.34	156	307	181	355	186	366	194	382	198	389
Dantu	5.07	415	400	435	417	442	426	448	431	452	435
Jurong	8.03	260	397	281	429	287	438	293	447	298	455
Danyang	9.58	210	382	228	415	236	420	240	437	247	449
Jiaxing	6.57	38	47	60	75	65	81	69	86	74	93
Jiashan	4.13	-132	-103	-119	-93	-113	-87	-110	-86	-105	-82
Pinghu	4.81	259	236	286	261	297	272	304	278	313	286
Haiyan	2.74	192	100	220	114	235	122	242	126	251	130
Haining	3.92	203	151	216	161	222	166	225	168	230	171
Tongxiang	4.42	222	186	247	207	257	216	263	221	271	227
Huzhou	6.02	-278	-318	-265	-303	-265	-299	-259	-296	-256	-293
Changxing	5.62	-89	-95	-82	-77	-72	-77	-69	-74	-66	-71
Anji	4.18	-71	-56	-56	-45	-54	-43	-51	-41	-46	-37
Deqing	3.11	-111	-65	-98	-58	-95	-56	-91	-54	-88	-52
Yuhang	5.27	-59	-59	-47	-47	-44	-44	-39	-39	-37	-37
Linan	3.06	-44	-26	-8	-5	2	1	12	7	21	12
Minhang	3.49	151	100	170	113	175	119	181	120	183	121
Jiading	4.29	275	224	294	240	299	244	306	249	310	252
Chuangsha	3.71	354	250	379	268	386	273	395	279	399	282
Nanhui	4.11	193	151	218	170	225	176	234	183	238	186
Qingpu	5.68	-60	-65	-36	-39	-29	-31	-21	-22	-16	-17
Songjiang	5.9	-235	-263	-211	-237	-205	-229	-196	-220	-191	-215
Jinshan	5.63	-84	-89	-60	-64	-54	-58	-47	-50	-43	-46
Fengxian	5.87	128	143	150	167	156	174	164	183	168	187
Baoshan	3.13	377	225	403	240	412	245	417	248	423	252
Chongming	3.73	286	203	310	219	316	224	321	228	329	233

Jiaxing (7.0 -93 kg C ha⁻¹ year⁻¹), Jiashan (12 -98 kg C ha⁻¹ year⁻¹), and Anji (30 -91 kg C ha⁻¹ year⁻¹). By contrast, these counties possessed relatively low SOC increase amount (19 -35 kg C ha⁻¹ year⁻¹, 26 -47 kg C ha⁻¹ year⁻¹, 22 -36 kg C ha⁻¹ year⁻¹, 13 -27 kg C ha⁻¹ year⁻¹, and 15 -25 kg C ha⁻¹ year⁻¹, respectively) in different atmospheric CO₂ concentration scenarios. The modeled result is in agreement with other studies, indicating air temperature is significantly and positively correlated with changes in soil respiration (Bond-Lamberty and Thomson, 2010), and a faster SOC turnover associated with higher temperatures could result in the loss of significant amounts of C stored in agricultural soils (Álvarez-Fuentes et al., 2012).

3.5. Uncertainty and limitations of model results

The uncertainties in the input parameters and forcing data propagate through the DNDC and cascade to the model estimates when applying the DNDC model at a regional scale (Li et al., 2004). In the study, although a digital soil database of 1:50,000 in the Tai-Lake region was used to drive the DNDC simulations. However, there are other uncertainty sources to affect our understanding of the SOC balance impacted by rising temperatures and elevated atmospheric CO₂.

First, county is used as the basic simulation unit because existing input data was often limited to a county level (e.g., management practice data), especially in China. Thus, uncertainties in estimates are affected by the inherent heterogeneities of

input for a specific county during the scaling-up process. For example, county level data in general management practices might not be able to capture the field-specific on-farm measures used to enhance crop yields. In addition, climate change is an important driver of SOC change in the Tai-Lake region in the period of 2001–2019. However, the meteorological data at county level were obtained from the nearest weather station and ignored the spatial heterogeneity of precipitation and temperature.

Second, the assumption of a 15% of aboveground crop residue returning to the soil across the whole Tai-Lake region during the periods of 2001–2019 might cause uncertainty. The value of 15% was the national average derived from the Agricultural Ministry (Tang et al., 2006). Actually, the fraction of above-ground crop residue returned to the field had a considerable discrepancy among different counties.

The third possible source of the modeling uncertainty is induced from the diversity of cropping systems in the study area. Although rice-wheat rotation is the dominant cropping systems in the Tai-Lake region, the rice-rapeseed and rice-cotton rotations also exist in a small area. As such, there is a certain degree of discrepancy between the cropping system represented in the model and that in reality. Remote sensing data, however, could potentially provide temporally and spatially explicit delineation of crop rotation systems.

Another limitation of this study arises from the complexity of feedback between the elevated CO₂ concentration and warming and the inability of the DNDC in capturing this feedback. Increase

Table 7

Average annual SOC change (AASC, kg C ha⁻¹ year⁻¹) and the total SOC change (TSC, Gg C) under different temperature scenarios by county level in the Tai-Lake region during the period of 2001–2019, China.

County	Area 10 ⁴ ha	T0.5		T1		T1.5		T2		T3		T4	
		AASC	TSC										
Wuxian	14.78	-119	-334	-134	-376	-137	-386	-156	-438	-186	-523	-205	-576
Zhangjiagang	2.54	74	36	66	32	64	31	55	27	40	19	29	14
Changshu	7.55	-103	-148	-120	-172	-123	-177	-134	-192	-152	-217	-164	-236
Taicnang	6.14	181	211	173	202	174	203	169	198	165	192	157	183
Kunshan	7.57	-100	-144	-118	-169	-123	-177	-136	-195	-151	-217	-165	-237
Wujiang	9.79	146	272	136	253	133	248	119	221	96	178	83	154
Wuxi	9.77	34	62	26	48	29	54	18	34	6	11	-8	-15
Jiangyin	8.69	102	168	91	150	89	147	81	133	70	115	58	96
Wujin	14.85	98	276	90	253	91	256	81	228	74	210	66	186
Jintan	7.1	189	255	176	238	177	238	170	229	156	210	145	195
Liyang	10.84	208	429	196	404	196	403	188	388	174	359	164	338
Yixing	10.34	162	317	149	292	149	292	142	279	122	239	104	205
Dantu	5.07	409	394	415	400	406	391	400	385	392	377	384	369
Jurong	8.03	257	392	261	399	247	377	237	361	212	324	193	294
Danyang	9.58	200	363	202	367	189	345	182	330	165	300	147	268
Jiaxing	6.57	31	39	15	19	7	9	-11	-14	-35	-44	-55	-69
Jiashan	4.13	-144	-113	-163	-128	-169	-133	-189	-147	-215	-169	-230	-180
Pinghu	4.81	259	236	250	229	251	229	243	222	238	217	232	212
Haiyan	2.74	197	103	186	97	186	96	176	92	161	84	148	77
Haining	3.92	200	149	187	139	177	132	165	123	153	114	129	96
Tongxiang	4.42	221	186	213	179	212	178	203	171	195	163	184	155
Huzhou	6.02	-284	-325	-300	-343	-307	-351	-321	-367	-351	-401	-375	-429
Changxing	5.62	-93	-99	-105	-112	-107	-114	-118	-126	-138	-147	-146	-156
Anji	4.18	-100	-80	-113	-90	-121	-96	-129	-103	-142	-113	-161	-128
Deqing	3.11	-113	-67	-123	-72	-133	-79	-144	-85	-154	-91	-185	-109
Yuhang	5.27	-61	-61	-71	-71	-81	-81	-92	-93	-100	-100	-123	-123
Linan	3.06	-44	-25	-43	-25	-35	-20	-34	-20	-37	-22	-67	-39
Minhang	3.49	149	99	138	91	133	88	123	81	106	70	89	59
Jiading	4.29	272	222	262	213	259	211	251	205	238	194	127	103
Chuangsha	3.71	353	249	346	244	345	244	339	239	331	234	322	227
Nanhui	4.11	190	149	160	140	176	138	168	131	154	121	139	109
Qingpu	5.68	-64	-69	-77	-83	-81	-87	-89	-96	-102	-110	-116	-125
Songjiang	5.9	-240	-269	-253	-283	-258	-288	-266	-297	-277	-310	-290	-325
Jinshan	5.63	-88	-94	-102	-109	-107	-115	-115	-123	-132	-141	-148	-158
Fengxian	5.87	126	140	115	128	112	124	103	115	87	97	73	81
Baoshan	3.13	381	227	369	220	371	221	371	221	362	216	358	213
Chongming	3.73	284	202	276	196	280	198	281	199	279	198	278	197

in CO₂ concentration leads to increase in air temperature due to its effects of radiative forcing (IPCC, 2013). As a result, elevated CO₂ concentration induced warming would affect SOC changes. However, this feedback has not been investigated in this study, while our focus is on the SOC balance between the potential carbon sink induced from CO₂ fertilization and potential carbon source derived from rising temperature. More comprehensively accounting for these effects would be our future research priority.

4. Conclusion

Based on the currently highest spatial resolution soil database, this study elucidates the counteracting effects between rising temperatures and CO₂ fertilization on SOC and the soil heterogeneity induced SOC variations for the entire Tai-Lake paddy region of China, using a process-based biogeochemistry model (DNDC). We found that the positive effect of carbon sink induced by CO₂ fertilization at the 2.0 times normal concentration increase rate could generally offset the negative effect of carbon source derived by rising temperature to 2.0 °C. The results indicate that the effects of rising temperatures and CO₂ fertilization on SOC in different paddy soil subgroups, sub-regions, and administrative areas are highly variable due to heterogeneity in soil properties and fertilizer use. This highlights the importance of incorporating the abovementioned heterogeneity into SOC modeling. Additionally, our results suggest that the overall positive effects of CO₂ fertilization on SOC are prone to outweigh the negative effects induced from warming in the study

region, which stress the key role of agro-ecosystems in regulating global carbon cycling and mitigating global warming.

Acknowledgements

We gratefully acknowledge support from the Foundation of National Natural Science Foundation of China (No. 41001126), the Natural Science Foundation of Fujian province in China (No. 2015J01154), and the Program for New Century Excellent Talents in University of Fujian Province of China (No. JA14097). Sincere thanks are also given to Professor Changsheng Li (University of New Hampshire, USA) for his valuable advice on use of the DNDC model.

References

- Abdalla, M., Kumar, S., Jones, M., Burke, J., Williams, M., 2011. Testing DNDC model for simulating soil respiration and assessing the effects of climate change on the CO₂ gas flux from Irish agriculture. *Global Planet. Change* 78, 106–115.
- Álvarez-Fuentes, J., Easter, M., Paustian, K., 2012. Climate change effects on organic carbon storage in agricultural soils of northeastern Spain. *Agr. Ecosyst. Environ.* 155, 87–94.
- Álvarez-Fuentes, J., Paustian, K., 2011. Potential soil carbon sequestration in a semiarid Mediterranean agroecosystem under climate change: Quantifying management and climate effects. *Plant Soil* 338, 261–272.
- Bond-Lamberty, B., Thomson, A., 2010. Temperature-associated increases in the global soil respiration record. *Nature* 464, 579–582.
- Booker, F.L., Miller, J.E., Fiscus, E.L., Pursley, W.A., Stefanski, L.A., 2005. Comparative responses of container- versus ground-grown soybean to elevated carbon dioxide and ozone. *Crop Sci.* 45, 883–895.

- Brar, B.S., Singh, K., Dheri, G.S., Kumar, B., 2013. Carbon sequestration and soil carbon pools in a rice–wheat cropping system: Effect of long-term use of inorganic fertilizers and organic manure. *Soil Till. Res.* 128, 30–36.
- Bu, J.F., 2013. Scale effects of dynamic simulation of paddy soil organic carbon in Tai-Lake region based on scenario analysis. Dissertation, Fujian Agriculture and Forestry University (in Chinese with English abstract).
- Chavas, D.R., Izaurrealde, R.C., Thomson, A.M., Gao, X.J., 2009. Long-term climate change impacts on agricultural productivity in eastern China. *Agr. Forest Meteorol.* 149, 1118–1128.
- China Meteorological Administration., 2011. China Meteorological Data Daily Value. China Meteorological Data Sharing Service System, Beijing, China. <http://cdc.cma.gov.cn/index.jsp>.
- Cole, V., Cerri, C., Minami, K., Mosier, A., Rosenberg, N., Sauerbeck, D., 1996. Agricultural options for mitigation of greenhouse gas emissions. In: Watson, R. T., Zinyowera, M.C., Moss, R.H. (Eds.), *Climate Change 1995: Impacts, Adaptation and Mitigation of Climate Change*. Cambridge University Press, Cambridge, UK, pp. 744–771.
- Coleman, K., Jenkinson, D.S., Crocker, G.J., Grace, P.R., Klir, J., Korschens, M., Poulton, P.R., Richter, D.D., 1997. Simulating trends in soil organic carbon in long-term experiments using RothC-26.3. *Geoderma* 81, 29–44.
- Fuhrer, J., 2003. Agroecosystem responses to combinations of elevated CO₂, ozone, and global climate change. *Agr. Ecosyst. Environ.* 97, 1–20.
- Gao, M.F., Qiu, J.J., Li, C.S., Wang, L.G., Li, H., Gao, C.Y., 2014. Modeling nitrogen loading from a watershed consisting of cropland and livestock farms in China using Manure-DNDC. *Agr. Ecosyst. Environ.* 185, 88–98.
- Gaston, G.G., Kolchugina, T., Vinson, T.S., 1993. Potential effect of no-till management on carbon in the agricultural soils of the former Soviet Union. *Agr. Ecosyst. Environ.* 45, 295–309.
- Gaumont-Guay, D., Black, T.A., Griffis, T.J., Barr, A.G., Jassal, R.S., Nesic, Z., 2006. Interpreting the dependence of soil respiration on soil temperature and water content in a boreal aspen stand. *Agr. Forest Meteorol.* 140, 220–235.
- Goglio, P., Grant, B.B., Smith, W.N., Desjardins, R.L., Worth, D.E., Zentner, R., Malhi, S. S., 2014. Impact of management strategies on the global warming potential at the cropping system level. *Sci. Total Environ.* 490, 921–933.
- Gottschalk, P., Smith, J.U., Wattenbach, M., Bellarby, J., Stehfest, E., Arnell, N., Osborn, T.J., Jones, C., Smith, P., 2012. How will organic carbon stocks in mineral soils evolve under future climate? Global projections using RothC for a range of climate change scenarios. *Biogeosciences* 9, 3151–3171.
- Gou, J., Zheng, X.H., Wang, M.X., Li, C.S., 1999. Modeling N₂O emissions from agriculture fields in Southeast China. *Adv. Atmos. Sci.* 16, 581–592.
- Houghton, R.A., Davidson, E.A., Woodwell, G.M., 1998. Missing sinks, feedbacks and understanding the role of terrestrial ecosystems in the global carbon balance. *Global Biogeochem. Cy.* 12, 25–34.
- Intergovernmental Panel on Climate Change., 1995. *Climate Change 1995: the Science of Climate Change. Contribution of Working Group I to the Second Assessment of the Intergovernmental Panel on Climate Change*. Cambridge University Press, Cambridge, UK and New York, NY, USA.
- Intergovernmental Panel on Climate Change., 2007. *Climate Change 2007: Synthesis Report. Summary for Policymakers*. Cambridge University Press, Cambridge, UK and New York, NY, USA.
- Intergovernmental Panel on Climate Change., 2013. *Climate Change 2013: Synthesis Report. Summary for Policymakers*. Cambridge University Press, Cambridge, UK and New York, NY, USA.
- Jastrow, J.D., Miller, R.M., Matamala, R., Norby, R.J., Boutton, T.W., Rice, C.W., Owensby, C.E., 2005. Elevated atmospheric carbon dioxide increases soil carbon. *Global Change Biol.* 11, 2057–2064.
- Kögel-Knabner, I., Amelung, W., Cao, Z.H., Fiedler, S., Frenzel, P., Jahn, R., Kalbitz, K., Kölbl, A., Schlotter, M., 2010. Biogeochemistry of paddy soils. *Geoderma* 157, 1–14.
- Leech, N.L., Barret, K.K.C., Morgan, G., 2008. *SPSS for Intermediate Statistics*. Lawrence Erlbaum Associates, New York, pp. 270.
- Li, Q.K., 1992. Paddy soil of China. China Science Press, Beijing, pp. 514 (in Chinese with English abstract).
- Li, C.S., 2000. Loss of soil carbon threatens Chinese agriculture: a comparison on agroecosystem carbon pool in China and the U.S. *Quaternary Sci.* 20, 345–350 (in Chinese with English abstract).
- Li, C.S., 2007a. Quantifying greenhouse gas emissions from soils: Scientific basis and modeling approach. *Soil Sci. Plant Nutr.* 53, 344–352.
- Li, C.S., 2007b. Quantifying soil organic carbon sequestration potential with modeling approach. In: Tang, H.J., Van Ranst, E., Qiu, J.J. (Eds.), *Simulation of Soil Organic Carbon Storage and Changes in Agricultural Cropland in China and its Impact on Food Security*. China Meteorological Press, Beijing, pp. 1–14.
- Li, C.S., Frolking, S., Frolking, T.A., 1992a. A model of nitrous oxide evolution from soil driven by rainfall events: I. Model structure and sensitivity. *J. Geophys. Res.* 97, 9759–9776.
- Li, C.S., Frolking, S., Frolking, T.A., 1992b. A model of nitrous oxide evolution from soil driven by rainfall events: II. Model applications. *J. Geophys. Res.* 97, 9777–9783.
- Li, C.S., Mosier, A., Wassmann, R., Cai, Z.C., Zheng, X.H., Huang, Y., Tsuruta, H., Boonjawan, J., Lantin, R., 2004. Modeling greenhouse gas emissions from rice-based production systems: Sensitivity and upscaling. *Global Biogeochem. Cy.* 18, GB1043. doi:<http://dx.doi.org/10.1029/2003GB002045>.
- Li, C.S., Salas, W., DeAngelo, B., Rose, S., 2006. Assessing alternatives for mitigating net greenhouse gas emissions and increasing yields from rice production in China over the next twenty years. *J. Environ. Qual.* 35, 1554–1565.
- Lin, Z.B., Zhang, R.D., 2012. Dynamics of soil organic carbon under uncertain climate change and elevated atmospheric CO₂. *Pedosphere* 22, 489–496.
- Liu, Q.H., Shi, X.Z., Weindorf, D.C., Yu, D.S., Zhao, Y.C., Sun, W.X., Wang, H.J., 2006. Soil organic carbon storage of paddy soils in China using the 1:1,000,000 soil database and their implications for C sequestration. *Global Biogeochem. Cy.* 20 doi:<http://dx.doi.org/10.1029/2006GB002731> GB3024.
- Lu, R.K., Shi, T.J., 1982. *Agricultural chemical manual*. China Science Press, Beijing, pp. 142 (in Chinese with English abstract).
- McLaughlan, K.K., 2006. Effects of soil texture on soil carbon and nitrogen dynamics after cessation of agriculture. *Geoderma* 136, 289–299.
- Pacey, J.G., DeGier, J.P., 1986. The factors influencing landfill gas production. In: *Energy from landfill gas. Proceeding of a conference jointly sponsored by the United Kingdom Department of Energy and the United States Department of Energy* (October 1986), pp. 51–59.
- Parton, W.J., Scurlock, J.M.O., Ojima, D.S., Gilmanov, T.G., Scholes, R.J., Schimel, D.S., Kirchner, T., Meentemeyer, J.C., Seastedt, T., Moya, E.G., Kamnalrut, A., Kinyamaro, J.I., 1993. Observations and modeling of biomass and soil organic matter dynamics for the grassland biome worldwide. *Global Biogeochem. Cy.* 7, 785–809.
- Parton, W.J., Scurlock, J.M.O., Ojima, D.S., Schimel, D.S., Hall, D.O., 1995. Impact of climate change on grassland production and soil carbon worldwide. *Global Change Biol.* 1, 13–22.
- Pathak, H., Li, C.S., Wassmann, H., 2005. Greenhouse gas emissions from Indian rice fields: calibration and upscaling using the DNDC model. *Biogeosciences* 2, 113–123.
- Peinetti, H.R., Menezes, R.S.C., Tiessen, H., Marin, A.M.P., 2008. Simulating plant productivity under different organic fertilization practices in a maize/native pasture rotation system in semi-arid NE Brazil. *Comput. Electron. Agr.* 62, 204–222.
- Shi, X.Z., Yu, D.S., Warner, E.D., Sun, W.X., Petersen, G.W., Gong, Z.T., Lin, H., 2006. Cross-reference system for translating between genetic soil classification of China and Soil Taxonomy. *Soil Sci. Soc. Am. J.* 70, 78–83.
- Six, J., Conant, R.T., Paul, E.A., Paustian, K., 2002. Stabilization mechanisms for soil organic matter: implications for C saturation of soils. *Plant Soil* 141, 155–176.
- Soil Survey Staff in USDA, 2010. *Keys to Soil Taxonomy*, 11th ed. USDA-Natural Resources Conservation Service, Washington, pp. 163–165.
- Sun, W.J., Huang, Y., Zhang, W., Yu, Y.Q., 2010. Carbon sequestration and its potential in agricultural soils of China. *Global Biogeochem. Cy.* 24 doi:<http://dx.doi.org/10.1029/2009GB003484> GB3001.
- Tang, H.J., Qiu, J.J., Van Ranst, E., Li, C.S., 2006. Estimations of soil organic carbon storage in cropland of China based on DNDC model. *Geoderma* 134, 200–206.
- Tonitto, C., David, M.B., Drinkwater, L.E., Li, C.S., 2007. Application of the DNDC model to tile-drained Illinois agroecosystems: model calibration, validation, and uncertainty analysis. *Nutr. Cycl. Agroecosyst.* 78, 51–63.
- Wang, M.X., Dai, A.G., Huang, J., Ren, L.X., Shen, R.X., Schutz, H., Rennenberg, H., Seiler, W., Rasmussen, R.A., Khalil, M.A.K., 1993. Sources of methane in China: rice fields, agricultural waste treatment, cattle, oil mines, and other minor sources. *Chin. J. Atmos. Sci.* 17 (1), 52–64 (in Chinese with English abstract).
- Wang, Y.H., Zhou, G.S., Wang, Y.H., 2007. Modeling responses of the meadow steppe dominated by *Leymus chinensis* to climate change. *Clim. Change* 82, 437–452.
- Xu, Q., Lu, Y.C., Liu, Y.C., Zhu, H.G., 1980. Paddy Soil of Tai-Lake Region in China. China Science Press, Shanghai, pp. 51–80 (in Chinese with English abstract).
- Xu, S.X., Shi, X.Z., Zhao, Y.C., Yu, D.S., Li, C.S., Wang, S.H., Tan, M.Z., Sun, W.X., 2011. Carbon sequestration potential of recommended management practices for paddy soils of China, 1980–2050. *Geoderma* 166, 206–213.
- Xu, S.X., Shi, X.Z., Zhao, Y.C., Yu, D.S., Wang, S.H., Sun, W.X., Li, C.S., 2012. Spatially explicit simulation of soil organic carbon dynamics in China's paddy soils. *Catena* 92, 113–121.
- Yu, D.S., Shi, X.Z., Wang, H.J., Sun, W.X., Warne, E.D., Liu, Q.H., 2007. National scale analysis of soil organic carbon stocks in China based on Chinese soil taxonomy. *Pedosphere* 17, 11–18.
- Yu, Y.Q., Zhang, W., Huang, Y., 2014. Impact assessment of climate change, carbon dioxide fertilization and constant growing season on rice yields in China. *Clim. Change* 124, 763–775.
- Zhang, L.M., Yu, D.S., Shi, X.Z., Weindorf, D.C., Zhao, L.M., Ding, W.X., Wang, H.J., Pan, J.J., Li, C.S., 2009a. Quantifying methane emissions from rice fields in the Taihu region, China by coupling a detailed soil database with biogeochemical model. *Biogeosciences* 6, 739–749.
- Zhang, L.M., Yu, D.S., Shi, X.Z., Weindorf, D.C., Zhao, L.M., Ding, W.X., Wang, H.J., Pan, J.J., Li, C.S., 2009b. Simulation of global warming potential (GWP) from rice fields in the Tai-Lake region, China by coupling 1:50,000 soil database with DNDC model. *Atmos. Environ.* 43, 2737–2746.
- Zhang, L.M., Yu, D.S., Shi, X.Z., Xu, S.X., Wang, S.H., Xing, S.H., Zhao, Y.C., 2012. Simulation soil organic carbon change in China's Tai-Lake paddy soils. *Soil. Till. Res.* 121, 1–9.
- Zhang, L.M., Yu, D.S., Shi, X.Z., Xu, S.X., Xing, S.H., Zhao, Y.C., 2014. Effects of soil data and simulation unit resolution on quantifying changes of soil organic carbon at regional scale with a biogeochemical process model. *PLoS ONE* 9 (2), e88622. doi:<http://dx.doi.org/10.1371/journal.pone.0088622>.
- Zhang, W., Yu, Y.Q., Sun, W.J., Huang, Y., 2007. Simulation of soil organic carbon dynamics in Chinese rice paddies from 1980 to 2000. *Pedosphere* 17 (1), 1–10.
- Zhang, Y., Wang, Y.Y., Su, S.L., Li, C.S., 2011. Quantifying methane emissions from rice paddies in Northeast China by integrating remote sensing mapping with a biogeochemical model. *Biogeosciences* 8, 1225–1235.
- Zhao, Y.C., Shi, X.Z., Weindorf, D.C., Yu, D.S., Sun, W.X., Wang, H.J., 2006. Map scale effects on soil organic carbon stock estimation in north China. *Sci. Soc. Am. J.* 70, 1377–1386.
- Zhao, G., Bryan, B.A., King, D., Luo, Z.K., Wang, E.L., Song, X.D., Yu, Q., 2013. Impact of agricultural management practices on soil organic carbon: simulation of Australian wheat systems. *Global Change Biol.* 19, 1585–1597.